

## 9. Electrically Excited and Permanent Magnet Synchronous Machines

### 9.1 Electrical Excitation Systems

The excitation system has to deliver the dc power  $P_f$  for the excitation of the rotor. Depending on the size of the synchronous machine, this equals from about 0.5 % (large machines in the MW-range) up to 3 % (small machines in the kW-range) of the rated machine power  $P_N$ .

$$P_f = U_f I_f \quad (9.1)$$

(i) At **line operation**, the terminal voltage of the synchronous machine is determined by the line. The consumption of reactive power is controlled via the exciting current  $I_f$ .

(ii) At **isolated operation**, the terminal voltage is maintained constant via the exciting current. This changes with variable load and stator current, especially because of the voltage drop at the synchronous reactance, where the voltage change at high reactive current is maximum, as it was shown in Chapter 8.

The **rated exciting voltage** (9.2) corresponds to the **rated exciting current**  $I_{fN}$ , what is important for operation at rated conditions (e.g.  $U_N, I_N, \cos\varphi_N = 0.8$ , over-excited).

$$U_{fN} = R_f I_{fN} \quad (9.2)$$

a) **High-Speed Excitation:**

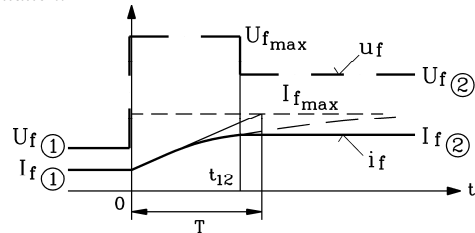


Fig. 9.1: **High-speed excitation:** In order to build up field as fast as possible, the exciting current is increased from its initial value  $I_{f1}$  to the final value  $I_{f2}$  by the ceiling voltage  $U_{fmax}$ .  $I_{f2}$  is obtained after the time  $t_{12}$ .

The exciting system must have a large enough voltage reserve  $U_{fmax} > U_{fN}$  to allow for a fast change of the exciting current at variable load conditions. The maximum voltage  $U_{fmax}$  of the excitation system is called **“ceiling voltage”**. It has the standardised designation  $U_{Ep}$ . If – starting from operation with the exciting current  $I_{f1}$  – the bigger new value  $I_{f2}$  shall be reached as fast as possible, the exciting current is increased by the maximum exciting voltage according to Fig. 9.1, until the desired value  $I_{f2}$  is obtained (**“high-speed excitation”**). Then, the voltage is reduced down to  $U_{f2} = R_f I_{f2}$ . Due to the inductance  $L_f$  and the resistance  $R_f$  of the rotor winding, the exciting current increases delayed by the **field no-load constant**  $T_f$ . At generator no-load (= stator winding at zero current), this time constant is:

$$T_f = L_f / R_f \quad (9.3)$$

Generally, the maximum possible exciting current  $I_{fmax} = U_{fmax}/R_f$  is larger than the thermal permissible continuous exciting current.

b) **High-Speed De-Excitation:**

If the synchronous machine is suddenly – e.g. as a result of a perturbation in the grid – disconnected from the line, the power switch opens and the stator current is zero. The terminal voltage rises up to the value of the no load voltage. At constant excitation and overexcited operation, this voltage is up to 30 % larger than the rated voltage, as shown in Section 9.2 by the no-load characteristic. To avoid this, the exciting current is decreased quickly (**“high-speed de-excitation”**). As the field constant is in the order of some seconds, hence, it is relatively large. So, it has to be reduced by an external resistance  $R_v$  (Fig. 9.2).

$$T_f^* = L_f / (R_f + R_v) = T_f / (1 + \frac{R_v}{R_f}) \quad (9.4)$$

**Example 9.1-1:**

At  $R_v = 9R_f$ ,  $T$  is reduced down to  $T_f^* = T_f/10$ .

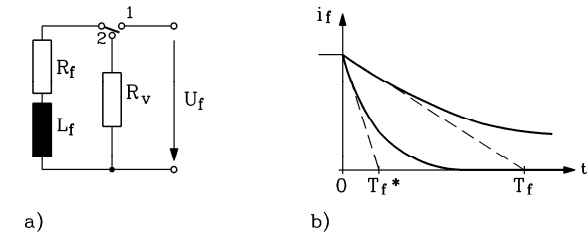


Fig. 9.2: **De-excitation** of the rotor: a) high-speed de-excitation resistance  $R_v$  (principal connection), b) decrease of the field current  $i_f$  without and with high-speed de-excitation resistance (time constants  $T_f$  and  $T_f^*$ )

c) **Excitation Systems:**

c1) **Converter Excitation:**

Generally, the three-phase line voltage is rectified via a controlled rectifier bridge (B6C-connection) to obtain a dc voltage of variable amplitude (Fig. 9.3), that is supplied to the rotor via two slip rings. Such **exciting systems** change the exciting voltage very fast. It was shown that the voltage ripple  $u_f(t)$  of the B6C-bridge contains six peaks per line period. This corresponds to voltage harmonics of 6<sup>th</sup>, 12<sup>th</sup>, ... order, hence 300 Hz, 600 Hz, ... at a 50 Hz line. The large inductance of the field winding  $L_f$  smoothes the current  $i_f(t)$ , so an almost ideal dc-current is obtained.

**Protective measures at operating disturbances:**

If e.g. a sudden short circuit occurs in the stator winding, the stator current amplitude changes suddenly and so does the amplitude of the air gap field. Due to that change of the rotating field it induces overvoltages in the rotor winding. The converter must be protected against these overvoltages via an external protective circuit (e.g. varistors).

c2) **DC Generators:**

Due to their excellent dynamic characteristic, the converter excitation has totally replaced the excitation method via **dc generators**. This formerly often used method consists of a main dc machine and an auxiliary exciting dc machine that are both mechanically coupled with the synchronous machine (Fig. 9.4). The armature current of the auxiliary dc machine is the field current of the main dc machine, whose armature current itself is the exciting current of the field winding. Due to this **cascading**, a high gain between field current of the auxiliary exciting machine  $I_{f,aux}$  and the exciting current of the synchronous machine  $I_f$  was obtained.

The field winding of the auxiliary dc machine is connected in parallel to its armature winding (see Chapter 11: dc machine). So, it is self-excited due to remanence according to the **electro-dynamic principle**. Therefore, running-up of the generator set after total line breakdown without an additional voltage is possible. Today, this is generally assured with small permanent magnet synchronous generators that are coupled to the synchronous machine. A considerable drawback of excitation by means of dc machines is the **poor dynamic performance**: The time constants of the field windings of the two dc machines add to the time constant of the synchronous rotor winding.

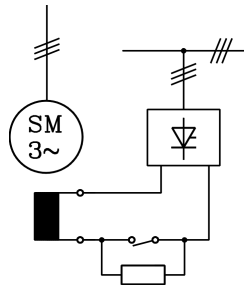


Fig. 9.3: Converter excitation with high-speed de-excitation resistance: A controlled rectifier supplies the rotor via two sliprings with variable dc voltage.

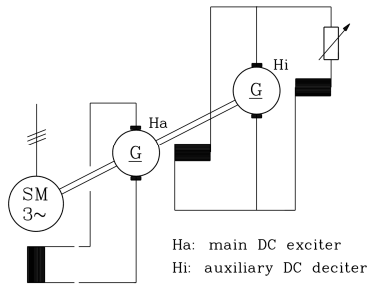


Fig. 9.4: Frequently used in the past: dc main and - auxiliary excitation machine for excitation of synchronous machines.

c3) Brushless Excitation:

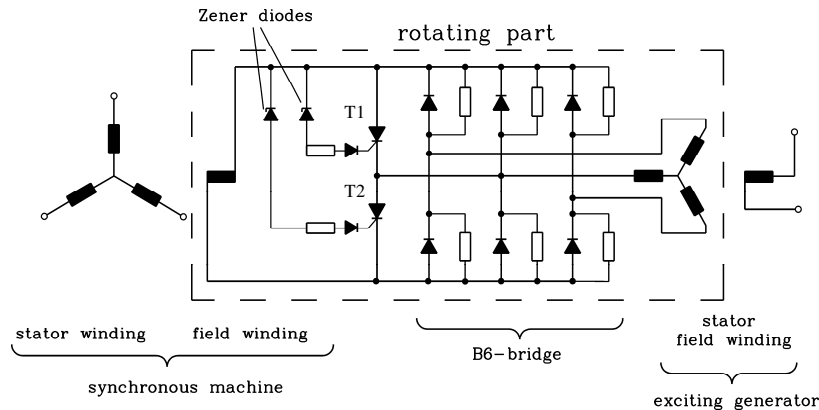


Fig. 9.5: Brushless excitation via outer rotor synchronous excitation generator and rotating B6-diode-bridge. Overvoltages that are induced in the rotor by the stator due to faults of the main machine ignite via the Zener diodes – depending on the polarity – the two thyristors T1 and T2. Thereby, the B6-bridge is protected from overvoltages.

Converter excitation and dc machines have the drawback of using carbon brush sliding contacts, either in the form of sliprings or at the commutators of dc machines. If a second, small synchronous machine is used as exciting machine (designed as **outer rotor machine**) and coupled to the large, main synchronous machine, the brush contacts and the sliprings can

be avoided (“**brushless excitation**”). The stator of the outer rotor generator consists of dc excited wound north and south poles that excite a static magnetic field. The three-phase winding is arranged in a slotted rotor lamination stack, as in the case of a slipring machine, where the winding terminals are connected to a B6-diode bridge that rotates along with the rotor. Thereby, the three-phase system, that is induced in the rotor winding by the static magnetic field, is rectified. The rectified rotor current flows in feeding cables that run in the shaft of the main machine to the rotor winding (Fig. 9.5). The amplitude of the induced rotor voltage and therefore the exciting current of the rotor of the main machine is varied via the dc field current of the exciting machine. However, again, the time constants of rotor and exciting machine add up and result in reduced dynamic performance. In addition, high-speed de-excitation is not possible, because no external resistance can be connected to the rotating voltage circuit. Details on **different concepts of field current control** of synchronous generators are explained in the lecture “Large Generators and High Power Drives”.

9.2 No-Load and Short-Circuit Characteristic

a) No-Load Characteristic:

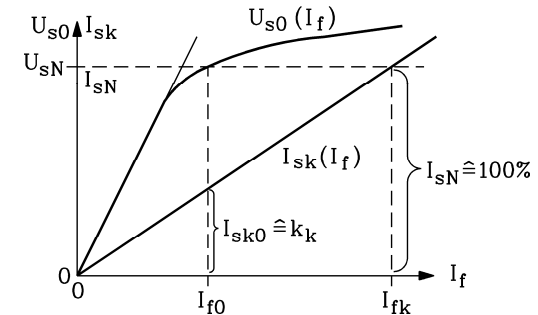


Fig. 9.6: No-load characteristic  $U_{s0}(I_f)$  and short-circuit characteristic  $I_{sk}(I_f)$  with consideration of saturation. The determination of the no-load/short-circuit ratio  $k_k$  (“short-circuit ratio”) is also shown.

If the synchronous machine is externally driven, the rotor excited and the stator terminals open, the back-e.m.f.  $U_p$  that is induced in the stator winding can be directly measured as “**no-load voltage  $U_{s0}$** ” (phase values) at the machine terminals. If, at constant machine speed, the exciting current  $I_f$  is increased from 0 up to its maximum value, the rotor field increases first linearly, and so does the no-load voltage. Only the air gap is magnetised by the field strength  $H_\delta$  because the permeability of the stator and the rotor iron is much bigger than  $\mu_0$  at low flux densities. The value of  $\mu_{Fe}$  is about  $3000\mu_0$  up to  $5000\mu_0$ . The magnetic field strength  $H_{Fe}$  in the iron is nearly zero. Applying AMPERE’s law to a closed field line (curve C) of the excited rotor, which crosses the air gap, we get:

$$\oint_C \vec{H} \cdot d\vec{s} = \Theta \Rightarrow H_\delta \delta + H_{Fe} \Delta F_e = N_{fPol} I_f \tag{9.5}$$

The air gap field has to concentrate in the stator teeth – and in the case of round rotor machines also in the rotor teeth – where it is about twice as large as in the air gap. Hence, at 0.7 T air gap flux density, the flux density in the teeth is about 1.4 T. Above 1.5 T, the iron begins to saturate,  $\mu_{Fe}$  decreases significantly,  $H_{Fe}$  can no longer be neglected and re-quires an additional magneto-motive force  $H_{Fe} \Delta F_e$  along the length of the iron paths  $\Delta F_e$  (e.g. tooth

length). Therefore, the air gap field  $H_\delta$  increases **sub-proportionally** with the exciting current and so does the no-load voltage (Fig. 9.6). In the case of typically rated air gap flux density of 1 T (about 2 T in the teeth), the iron part requires about 30 % to 50 % of the total required magneto-motive force, depending on the design.

b) Short-circuit Characteristic:

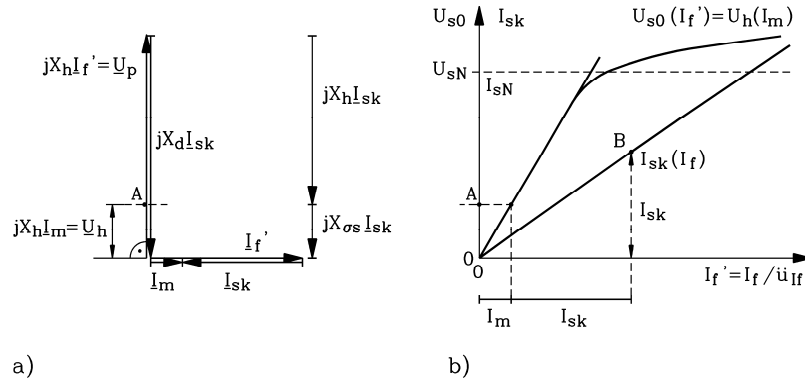


Fig. 9.7: Graphic determination of the short-circuit characteristic  $I_{sk}(I_f)$  from the a) phasor diagram for continuous short-circuit and b) the no-load characteristic  $U_h(I_m)$  of the machine.

If the stator winding is shorted at **constant speed** and variable excitation, the **steady state short-circuit current**  $I_{sk}$  flows. According to the phasor diagram of Fig. 9.7a,  $I_f'$  and  $I_{sk}$  have opposite phase angles, if  $R_s = 0$  is assumed. Stator and rotor field almost cancel each other. Only a small residual field remains in the air gap. It corresponds to the magnetising current  $I_m$  and induces the small internal voltage  $U_h$  into the stator winding. This voltage covers the voltage drop of  $I_{sk}$  and at the stator leakage reactance  $X_{os}I_{sk}$ . This small air gap field of about 0.1 ... 0.15 T does not saturate the iron (operating point A in Fig. 9.7b), even if exciting and stator current have values significantly larger than their rated current, resulting in short-circuit point B. Therefore the **stator short-circuit current** increases **linear** with increasing exciting current, giving a linear **short-circuit characteristic**  $I_{sk}(I_f)$  (Fig. 9.6).

c) No-Load-Short-Circuit-Ratio:

If the influence of the stator resistance is neglected ( $R_s = 0$ ), the following simple correlation for **experimental determination of the synchronous reactance**  $X_d$  is obtained. According to Fig. 9.7a), the absolute value of the steady short-circuit current  $I_{sk}$  is:

$$I_{sk} = U_p / X_d \quad (9.6)$$

If the field is excited by the “no-load exciting current”  $I_{f0}$ , the no-load voltage is equal to the rated voltage ( $U_{s0} = U_{sN}$ , Fig. 9.6). In this case, the short-circuit current is  $I_{sk0}$ :

$$I_{sk0} = \frac{U_p(I_{f0})}{X_d} = \frac{U_{sN}}{X_d} \quad (9.7)$$

Hence, the **measured value of the synchronous reactance** is:

$$X_d = \frac{U_{sN}}{I_{sk0}} \quad (9.8)$$

If the synchronous reactance is given as per unit of the rated impedance  $Z_N = U_{sN}/I_{sN}$  (9.9), using the correlation (9.10) that can be seen from Fig. 9.6, we get:

$$x_d = \frac{X_d}{Z_N} = \frac{U_{sN}}{I_{sk0}} \cdot \frac{I_{sN}}{U_{sN}} = \frac{I_{sN}}{I_{sk0}} = \frac{I_{fk}}{I_{f0}} \quad (9.9)$$

$$\frac{I_{sN}}{I_{sk0}} = \frac{I_{fk}}{I_{f0}} \quad (9.10)$$

The “**short-circuit exciting current**”  $I_{fk}$  is the field current required for the stator current in the shorted stator winding to reach the value of rated current.

**Result:**

The per-unit synchronous reactance  $x_d$  equals the ratio of the short-circuit and no-load exciting currents. The reciprocal value is called “**no-load/short-circuit-ratio**”  $k_K = 1/x_d$  (Fig. 9.6).

$$k_K = \frac{I_{f0}}{I_{fk}} = \frac{I_f(U_s = U_{sN}, I_s = 0)}{I_f(U_s = 0, I_s = I_{sN})} = \frac{1}{x_d} \quad (9.11)$$

As  $I_{f0}$  is larger for a saturated than an unsaturated machine, the “**saturated no-load-short-circuit-ratio**” is larger than the unsaturated one, or – expressed inversely – the saturated synchronous reactance is smaller than the unsaturated one:

$$x_{d,sat} < x_{d,unsat} \quad (9.12)$$

d) Magnitude of the Per-Unit Synchronous Reactance:

The **synchronous reactance**  $X_d$  is mainly determined by the magnetising inductance  $X_h$  of the air gap field. It is therefore proportional to  $N_s^2 \tau_p / \delta$ .

d1) Turbo Generators in Thermal Power Plants:

Big turbo generators are mostly two-pole machines. They generate their high torque via a large stator electric loading and hence a high rated current  $I_N$ , as the air gap field is limited by saturation. So, the rated impedance  $Z_N = U_N/I_N$  is very small. Furthermore, the pole pitch  $\tau_p$  is large due to only two poles ( $2p = 2$ ). Accordingly, turbo generators have a large per-unit synchronous reactance  $X_d/Z_N$ , and a small no-load-short-circuit ratio, e.g.  $k_K = 0.5$ . According to Chapter 8, a large synchronous reactance reduces the breakdown torque, so **turbo generators** have only a small static stability margin. They are operated with controlled exciting current for stable operation. By designing a big air gap  $\delta$  in the order of several cm, the synchronous reactance is kept small. This increases the demand of exciting current according to (9.5), so intensive cooling of the rotor winding is required.

d2) Salient Pole Synchronous Machines:

**Hydropower generators** rotate with small speed. Thus, they have a large number of poles and a small pole pitch. Therefore, the synchronous reactance is small. The **no-load-short-circuit ratio** ranges typically from 0.8 to 1.2; the static stability is large enough for standard operation.

### d3) Permanent Magnet Synchronous Machines:

The magnets of **Permanent Magnet Synchronous Machines** are often glued onto the rotor ("surface magnets"). The value of  $\mu_{rel}$  of the permanent magnets is almost 1. So, for the stator field crossing the air gap and the magnets, the low magnet permeance enlarges the magnetically effective "air gap". Therefore, the synchronous reactance is small.

|                                  | Pole number $2p$ | Synchronous reactance $x_d/p.u.$ |
|----------------------------------|------------------|----------------------------------|
| Turbo generators                 | 2                | 2.0                              |
| Salient pole machines            | $\geq 4$         | 0.8 ... 1.2                      |
| PM machines with surface magnets | $\geq 4$         | 0.3 ... 1.0                      |

Table 9.1: Typical values for per-unit synchronous reactance  $x_d$

#### Example 9.2-1:

No-load and short-circuit characteristic of a turbo generator according to Fig. 9.6 yield a value  $k_k = 0.43$  and  $x_d = 1/0.43 = 2.32$  p.u.

### 9.3 Electrically Excited Synchronous Machines with Damper Winding

Synchronous machines suitable for line-operation need a **damper winding**. This winding is arranged as sections of a **short-circuit cage** in additional slots in the pole shoes of salient pole machines or as **complete cage** in the case of round rotor machines (Fig. 9.8). At a sudden change of load, in the stable operating point A ( $-M_e, \vartheta_0$ ) of the  $M_e(\vartheta)$ -characteristic, the rotor of the synchronous machine without damper winding will oscillate undamped with the natural frequency given by equation (9.13) (Chapter 8) (Fig. 9.10a).  $J$  is the polar momentum of inertia of the coupled machine set.

$$f_e = \frac{1}{2\pi} \sqrt{\frac{p \cdot |c_{\vartheta}|}{J}} \quad (9.13)$$

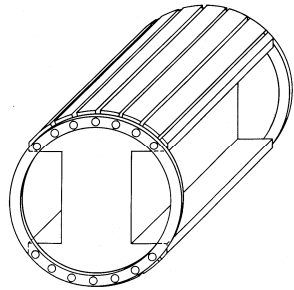


Fig. 9.8: Sections of damper cage of a two-pole salient pole machine in pole shoes.

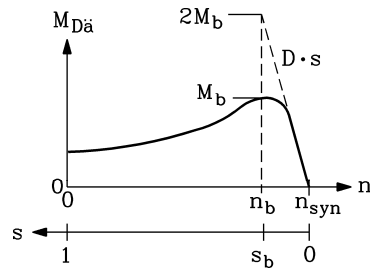


Fig. 9.9: Asynchronous torque of the damper cage. At synchronous operation, of  $s = 0$ , hence it has then no electromechanical effect.

The damping due to the stator resistance losses, friction in the bearings etc. is small. The oscillation is sinusoidal, if the amplitude  $\Delta M_e$  is small and hence linearisation of the  $M_e(\vartheta)$ -characteristic is permissible. The equivalent spring constant  $c_{\vartheta} (< 0)$  is obtained by linearisation of  $M_e(\vartheta)$ . Its magnitude depends on the chosen operating point A. In the stable range of  $|\vartheta| \leq \pi/2$ , it has a negative value (Fig. 9.10b).

$$|\Delta M_e| = |c_{\vartheta}(\vartheta - \vartheta_0)| \quad (9.14)$$

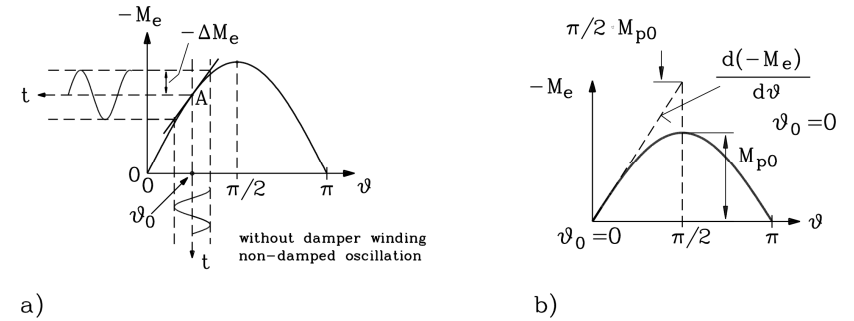


Fig. 9.10: Sudden load change of a round rotor synchronous machine in the operating point A without damper cage: a) undamped oscillation at the stationary operating point A ( $\vartheta = \vartheta_0$ ), b) equivalent spring constant  $c_{\vartheta}$  at no-load operating point ( $M_e = 0, \vartheta_0 = 0$ ):  $c_{\vartheta} = dM_e/d\vartheta = -M_{p0}$

The average speed  $\bar{n} = n_{syn}$  is constant. However, a sinusoidal oscillation is added, so  $\Omega_m(t) = 2\pi n(t)$  changes with time. The oscillation causes positive and negative displacement between rotor and stator rotating field, thereby causing a slip that changes its sign periodically. Therefore, **damping currents** are caused in each of the bars of the damper cage, which generate an asynchronous torque with the rotating field that counteracts the oscillation and causes it to decay. This asynchronous torque damps the oscillation of the rotor against the stator field. The oscillation decays within short time. The **asynchronous damper torque**  $M_{D\dot{a}}(s)$  according to Fig. 9.9 is of same nature as in induction machines. Due to the small slip  $s$ , it can be linearly approximated around the operating point  $s = 0$  using KLOSS's formula (Chapter 5).

$$M_{D\dot{a}}(s) \approx \frac{2M_b}{s_b} s = D \cdot s \quad \text{where} \quad s = \frac{\Omega_{syn} - \Omega_m}{\Omega_{syn}} = -\frac{\Delta\Omega_m}{\Omega_{syn}} \quad \text{and} \quad D = \frac{2M_b}{s_b} \quad (9.15)$$

Equation (9.15) is combined with the equation of motion.  $M_e$  and  $M_{D\dot{a}}$  are linearised in the operating point A:  $c_{\vartheta} = -|c_{\vartheta}| < 0$

$$J \frac{d\Omega_m}{dt} = M_e - M_s + M_{D\dot{a}} \quad \text{linearised:} \quad J \frac{d\Omega_m}{dt} = c_{\vartheta}(\vartheta - \vartheta_0) + D \cdot s \quad (9.16)$$

During the oscillation, the load angle changes with time:

$$\vartheta(t) = \vartheta_0 + p \int_0^t (\Omega_m(t) - \Omega_{syn}) dt \quad (9.17)$$

The deviation of the load angle from the steady-state value is:

$$\vartheta(t) - \vartheta_0 = \Delta\vartheta(t) \quad (9.18)$$

$$\frac{d^2\Delta\vartheta}{dt^2} = p(\Omega_m - \Omega_{syn}) = p \cdot \Delta\Omega_m = -p \cdot s \cdot \Omega_{syn}, \quad \frac{d^2\Delta\vartheta}{dt^2} = p \frac{d\Omega_m}{dt} = p \frac{d\Delta\Omega_m}{dt} \quad (9.19)$$

Using (9.18) and (9.19), the linearised equation (9.16) becomes a second order linear differential equation with constant coefficients:

$$\frac{J}{p} \Delta \dot{\vartheta} + \frac{D}{p \Omega_{syn}} \Delta \dot{\vartheta} + |c_{\vartheta}| \Delta \vartheta = 0 \quad (9.20)$$

The solution at initial condition  $\Delta \vartheta(0) = \Delta \vartheta_0$  is a damped oscillation:

$$\Delta \vartheta(t) = \vartheta(t) - \vartheta_0 = \Delta \vartheta_0 \cdot e^{-\alpha t} \cdot \cos(2\pi f_e' t) \quad (9.21a)$$

$$\alpha = \frac{D}{2J\Omega_{syn}} = \frac{M_b}{J\Omega_{syn}s_b} \quad f_e' = \frac{\sqrt{(2\pi f_e)^2 - \alpha^2}}{2\pi} \quad (9.21b)$$

#### Result:

The oscillation of the rotor decays due to the damper winding with the time constant  $1/\alpha$ . The frequency  $f_e'$  of the damped oscillation is slightly smaller than the frequency  $f_e$  of undamped oscillation (Fig. 9.11).

In the no-load operating point ( $M_e = 0$ ,  $\vartheta_0 = 0$ , Fig. 9.10b) the result can also be expressed using the rated acceleration time  $T_J$  (9.22) and  $p\Omega_{syn} = \omega_N$ .

$$T_J = \frac{J \cdot \Omega_{syn}}{M_N} \quad (9.22)$$

$$f_e = \frac{1}{2\pi} \sqrt{\frac{\omega_N}{T_J} \cdot \frac{M_{p0}}{M_N}}, \quad f_e' = \frac{1}{2\pi} \sqrt{\frac{\omega_N}{T_J} \cdot \frac{M_{p0}}{M_N} - \left( \frac{1}{s_b T_J} \cdot \frac{M_b}{M_N} \right)^2}, \quad \alpha = \frac{1}{s_b T_J} \cdot \frac{M_b}{M_N} \quad (9.23)$$

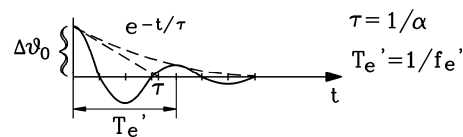


Fig. 9.11: Decay of the load angle oscillation due to damping by a damper cage

#### Example 9.3-1:

Data of a big synchronous machine: 100 MW, 50 Hz rated frequency:

- rated acceleration time:  $T_J = 10$  s,
- synchronous breakdown torque:  $M_{p0}/M_N = 1.5$ ,
- asynchronous breakdown torque of the damper cage:  $M_b/M_N = 1.4$ ,
- breakdown slip of the damper cage:  $s_b = 20\%$ .

At the no-load working point ( $M_e = 0$ ,  $\vartheta_0 = 0$ ) WITHOUT damper cage, the machine oscillates with the following natural frequency:

$$f_e = \frac{1}{2\pi} \sqrt{\frac{2\pi \cdot 50}{10} \cdot 1.5} = \underline{\underline{1.09 \text{ Hz}}}$$

If the oscillation is damped by a damper cage, the value of the natural frequency of oscillation is:

$$f_e' = \frac{1}{2\pi} \sqrt{\frac{2\pi \cdot 50}{10} \cdot 1.5 - \left( \frac{1}{0.2 \cdot 10} \cdot 1.4 \right)^2} = \underline{\underline{1.087 \text{ Hz}}}$$

The oscillation decays to  $1/e$  within the time constant  $\tau = 1/\alpha = 10 \cdot 0.2 / 1.4 = \underline{\underline{1.43 \text{ s}}}$ .

#### 9.4 Influence of the Damper Winding at Unbalanced Load and Harmonics

If the three phase currents do not have the same amplitude and/or a phase shift different to  $120^\circ$ el. (Fig. 9.12), the **load** of the electric rotating field machine is **unbalanced**. This is called “**unbalanced load**” (“**asymmetric load**”, “**load unbalance**”). The “phasor diagram” of the three complex phase current phasors is not symmetrical (Fig. 9.13). **Two** rotating fields are generated in the air gap of the ac machine – one positive and one negative sequence fundamental. Generally, both rotating fields have different amplitudes and **opposite direction of rotation**.

The existence of these two counterrotating fundamentals is explained using **symmetrical components**. The three arbitrarily chosen current phasors  $\underline{I}_U$ ,  $\underline{I}_V$ ,  $\underline{I}_W$  can be expressed as geometric sum of the phasors of three symmetric subsystems,

- one **positive sequence system** (r.m.s. current value  $I_1$ ),
- one **negative sequence system** (r.m.s. current value  $I_2$ ) and
- one **zero sequence system** (r.m.s. current value  $I_0$ ).

Within one subsystem, the three phase currents have the same rms value. In the positive and the negative sequence system, the value of the phase angle between the phase currents is  $120^\circ$ el., it is **zero** in the zero sequence system (name!). The phase sequence in the negative sequence system is **opposite** to the one in the positive sequence system (name!), hence it is U-W-V instead of U-V-W.

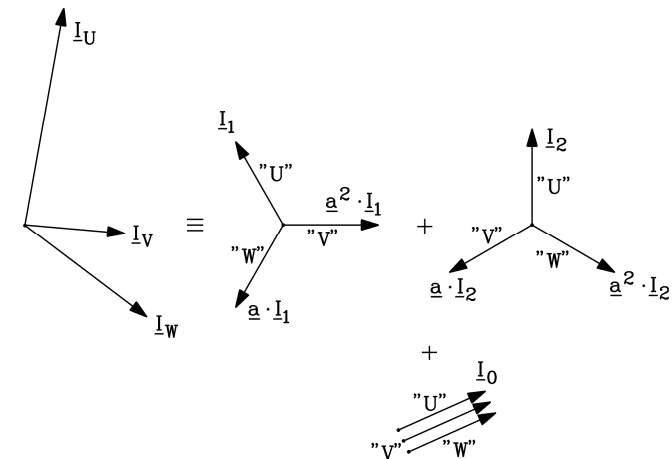


Fig. 9.12: An arbitrarily **unbalanced** three phase system  $\underline{I}_U$ ,  $\underline{I}_V$ ,  $\underline{I}_W$  can be decomposed into three symmetrical subsystems, which are the positive, the negative and the zero sequence system, as the graphical addition of the phasors of this figure shows (Please verify by yourself using set square and pencil!).

Multiplication of a phasor with

$$\underline{a} = e^{j2\pi/3} \quad (9.24)$$

causes a rotation of that phasor by  $120^\circ$  in mathematical positive rotational direction.

**Positive sequence system:**  $\underline{I}_{1U} = \underline{I}_1, \underline{I}_{1V} = \underline{a}^2 \cdot \underline{I}_1, \underline{I}_{1W} = \underline{a} \cdot \underline{I}_1$

**Negative sequence system:**  $\underline{I}_{2U} = \underline{I}_2, \underline{I}_{2V} = \underline{a} \cdot \underline{I}_2, \underline{I}_{2W} = \underline{a}^2 \cdot \underline{I}_2$

**Zero sequence system:**  $\underline{I}_{0U} = \underline{I}_0, \underline{I}_{0V} = \underline{I}_0, \underline{I}_{0W} = \underline{I}_0$

Using Fig. 9.12, the currents (rms values) of the three unsymmetrical current phasors are obtained:

$$\underline{I}_U = \underline{I}_1 + \underline{I}_2 + \underline{I}_0 \quad (9.25)$$

$$\underline{I}_V = \underline{a}^2 \underline{I}_1 + \underline{a} \underline{I}_2 + \underline{I}_0 \quad (9.26)$$

$$\underline{I}_W = \underline{a} \underline{I}_1 + \underline{a}^2 \underline{I}_2 + \underline{I}_0 \quad (9.27)$$

The inversion of equations (9.25) – (9.27) gives the equations for the determination of the r.m.s. values of positive, negative and zero sequence system  $\underline{I}_1, \underline{I}_2, \underline{I}_0$  from the phasors

$$\underline{I}_U, \underline{I}_V, \underline{I}_W.$$

$$\underline{I}_1 = (\underline{I}_U + \underline{a} \underline{I}_V + \underline{a}^2 \underline{I}_W) / 3 \quad (9.28)$$

$$\underline{I}_2 = (\underline{I}_U + \underline{a}^2 \underline{I}_V + \underline{a} \underline{I}_W) / 3 \quad (9.29)$$

$$\underline{I}_0 = (\underline{I}_U + \underline{I}_V + \underline{I}_W) / 3 \quad (9.30)$$

a) *Special Case of Symmetric Current System:*

Symmetric current system:  $\underline{I}_U, \underline{I}_V = \underline{a}^2 \underline{I}_U, \underline{I}_W = \underline{a} \underline{I}_U.$

Due to  $\underline{a}^3 = 1$ , it is derived from (9.28) – (9.30) that it is  $\underline{I}_1 = \underline{I}_U, \underline{I}_2 = 0, \underline{I}_0 = 0.$

b) *General Case of Asymmetric Current System:*

Large synchronous generators are generally star-connected. Applying *KIRCHHOFF*'s law (9.31) for the current in the star point, it becomes clear that a zero sequence system according to (9.30) can *not* be generated.

$$\underline{I}_U + \underline{I}_V + \underline{I}_W = 0 \quad (9.31)$$

Hence, only positive and negative sequence system remain. The **positive sequence system** corresponds to the case of symmetric currents in the three phase winding (as discussed in a)), which excite a rotating field rotating into the same direction as the rotor, thereby generating the constant synchronous torque  $M_e$  as discussed in Chapter 8.

The **negative sequence system** supplies the three phases of the stator winding with opposite phase sequence. This corresponds – as in the case of interchange of two terminals of the three phase winding – to a reversal of the direction of rotation of the rotating field. This **inverse air gap field** is magnetised by the three phase current system  $\underline{I}_2$ . Relatively to the rotor, it rotates with the speed:

$$v_{syn}(-v_{syn}) = 2v_{syn} = 2(2f\tau_p) = 2(2f)\tau_p \quad (9.32)$$

Hence, each north and each south pole of this inverse field induces the rotor winding with the frequency  $2f$ . The induced currents generate with the positive sequence field a pulsating

torque that pulsates with the frequency  $2f$  but has an average value of zero. It excites torsional vibrations within the machine.

Remark:

If the stator winding is delta-connected, a zero sequence current can flow as **delta current** in the three phases. It generates a standing, pulsating field with the pole number  $6p$  (see lecture: *CAD and System Dynamics of Electrical Machines*). This field induces currents in the damper winding and is damped in turn by these damping currents (see c)).

c) *Damping of the Negative Sequence Field:*

Due to the speed  $2v_{syn}$  relative to the rotor, the negative sequence field has a slip of  $s = 2$ . Therefore, it induces voltages in the damper bars with the frequency  $2f$ , that result in large damping currents. According to the theory of induction machines (see phasor diagram in Chapter 5), the air gap field of the damper current system  $\underline{I}'_D$  is almost opposite to the field of the negative sequence stator current system. Hence, the absolute value of the resultant magnetising current  $\underline{I}_{2m} = \underline{I}_2 + \underline{I}'_D$  is very small. That means, the resultant negative sequence field (magnetised by  $\underline{I}_{2m}$ ) is damped to very small residual values by the damping currents.

d) *Damping of Stator Field Harmonics:*

The stator field harmonics with ordinal number  $\nu$  of the positive sequence system have relative to the rotor the speed  $v_{syn}/\nu - v_{syn}$ , those of the negative sequence system  $v_{syn}/\nu + v_{syn}$ . So these harmonics induce the damper cage, causing currents to flow in the damper cage. These currents excite fields in the air gap, which are almost opposite to the stator harmonic fields, thereby damping the harmonic fields effectively.

## 9.5 Permanent Magnet Synchronous Machines

Instead of being electrically excited, the rotor can also be excited by permanent magnets to generate a constant rotor field (Fig. 9.13: Six pole permanent magnets glued onto the rotor surface).

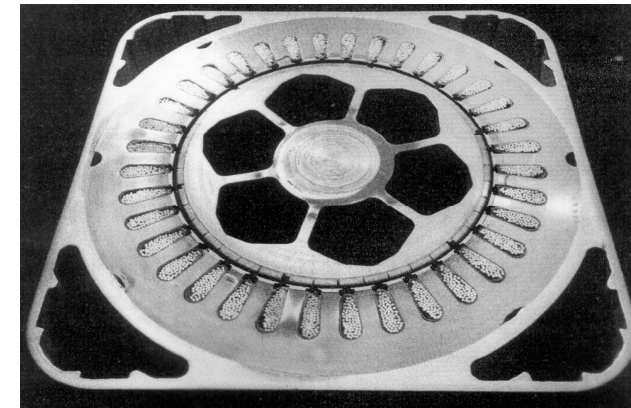


Fig. 9.13: Cross sectional cut of a permanent magnet machine with six poles. The surface mounted magnets can be easily seen in the rotor.

9.5.1 Characteristics of Permanent Magnets

a) Material Characteristics:

Permanent magnets are materials, where the magnetic dipole momentums in the small sub-domains of the crystalline material cause a residual magnetic polarisation  $J_M$ , even at absence of an external magnetic field. If exposed to an external field  $H_M$ , the dipole momentums aligns with the external field  $H_M$  with a certain delay. A hysteresis curve  $J_M(H_M)$  is obtained. In the case of very high field  $H_M$ , all dipoles are oriented into direction of  $H_M$ . So, the maximum polarisation  $\pm J_s$  occurs: the material is "saturated". The resultant external magnetic flux density as expressed by (9.33) can be measured:

$$\vec{B}_M = \mu_0 \vec{H}_M + \vec{J}_M \tag{9.33}$$

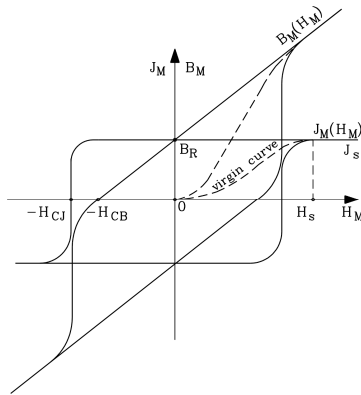


Fig. 9.14: Typical  $J_M(H_M)$ - and  $B_M(H_M)$ -hysteresis-characteristic of a rare-earth permanent magnet. The  $B_M(H_M)$ -characteristic is obtained by addition of  $B_M = \mu_0 H_M$  to the  $J_M(H_M)$ -characteristic.

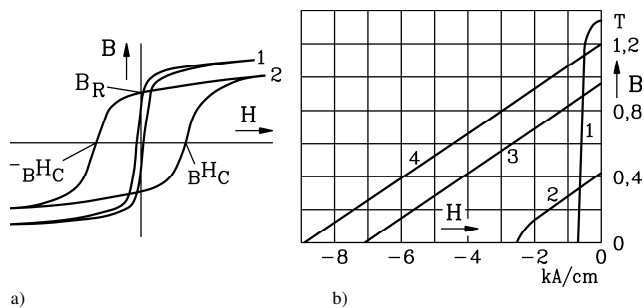


Fig. 9.15: a) (1) Soft and (2) hard magnetic material  $B(H)$ -characteristics, b)  $B(H)$ -characteristic of permanent magnets in the second quadrant of the  $B$ - $H$ -plane: (1): Al-Ni-Co magnet, (2): Ba-Ferrite magnet; rare-earth magnets: (3):  $Sm_2Co_{17}$ , (4): NdFeB (characteristics at 20°C)

After switching off of the external field, the **remanence flux density**  $B_R = J_M(H_M = 0) = J_R$  remains. Fig. 9.14 shows the  $J_M(H_M)$ -hysteresis curve and the resultant  $B_M(H_M)$ -characteristic (hysteresis curve) of the magnet, which is obtained by superposition of the  $J_M(H_M)$ -curve and

the straight line  $B_M = \mu_0 H_M$  according to (9.33). Therefore, two **coercive field strengths**  $H_C$  are distinguished:

- a) At  $\pm H_{CB}$ , the resultant external magnetic flux density  $B_M$  is zero.
- b) At  $\pm H_{CJ}$ , the magnetic polarisation  $J_M$  in the magnets has been reduced down to zero by reversion of polarity of the sub-domain dipoles.

b) Permanent Magnet Materials:

Three classes of permanent magnet materials ("**hard magnetic materials**") are used (Fig. 9.15b):

- **aluminium-nickel-cobalt magnets** AlNiCo with a high value  $B_R$ , but a low value of  $H_{CB}$ ,
- **ferrite**, e.g. barium-ferrite, with a significantly lower value of  $B_R$ , but higher value of  $H_{CB}$ ,
- **rare-earth magnets** (e.g. Samarium-Cobalt or Neodymium-Iron-Boron) with high values of both  $B_R$  and  $H_{CB}$ .

Fig. 9.15a shows the  $B(H)$ -hysteresis characteristic of a typical permanent magnet schematically and compares it with a soft-magnetic material, e.g. iron. With soft-magnetic materials, the values of  $B_R$  and  $H_C$  should be very small, to allow for low hysteresis losses when submitted to an alternating field. However, for hard-magnetic materials the values of  $B_R$  and  $H_C$  are large. Therefore, they are only suited for dc applications.

c) Demagnetisation:

The remanence flux density and the coercive field strength both decrease with **increasing temperature**, except in the case of ferrite materials, where the coercive field strength increases with increasing temperature. For the design of permanent magnet machines, it must be considered that the magnets may be permanently demagnetised in the external field of the stator coils, if the external field is opposing the field of the permanent magnets and exceeds a critical value. Such detailed questions are discussed in the lecture "*Motor Development for Electrical Drive Systems*".

9.5.2 Permanent Magnet Synchronous Motors

Today, expensive, but high-quality rare-earth magnets are increasingly used, because they can generate a high flux density in the air gap of an electric machine **WITHOUT** consuming energy and thereby generating losses. They increase the efficiency of an electric machine and reduce its heating. However, the excitation cannot be varied, and the power factor cannot be adjusted. Therefore permanent magnet synchronous machines are mostly used as small power motors, whereas large synchronous generators are electrically excited. Almost all permanent magnet motors are operated via inverters as variable speed drives.

Motors with both permanent magnets and damper cage in the rotor can be asynchronously started, and are used as special high-speed drives with speed up to typically 24 000 /min e.g. in the textile industry. Motors without damper cage as shown in Fig. 1.3a are used not only as **variable speed drives for machine tool and other production machine applications**, but also as large low speed, gearless direct drives for marine propulsion with power up to about 20 MW (!) or for wind generators.

If the  $B(H)$ -hysteresis-characteristic of ferrite and rare-earth magnets in the 2<sup>nd</sup> quadrant is assumed to be a straight line according to Fig. 9.15b, the slope corresponds with a good approximation to  $\mu_M = \mu_0$  (Fig. 9.14). If flux density and field strength inside the magnets are denoted  $B_M$  and  $H_M$ , it is:

$$B_M \cong B_R + \mu_0 H_M \tag{9.34}$$

Hence, rare-earth and ferrite-magnets show the same magnetic permeance as air towards external magnetic fields, because the differential permeability  $\mu_{diff} = dB/dH$  is about  $\mu_0$ . The magnetic field in the air gap – excited by permanent magnets – is determined by AMPERE's law. At no-load ( $I_s = 0$ ), the ampere-turns  $\Theta$  are zero. If the leakage flux between two neighbouring magnets is neglected and the iron assumed to be of infinite permeability ( $\mu_{Fe} \rightarrow \infty$ ), it is (Fig. 9.16):

$$2(H_\delta \delta + H_M h_M) = \Theta = 0 \tag{9.35}$$

With the surface mounted magnets the flux is  $\Phi = B_M A_M = B_\delta A_\delta$  and considering that the cross sectional areas of magnet and air gap are the same ( $A_M = A_\delta$ ), it is  $B_M = B_\delta$ . From (9.35), it is derived:

$$B_\delta = \mu_0 H_\delta = -\mu_0 \frac{h_M}{\delta} H_M = B_M \tag{9.36}$$

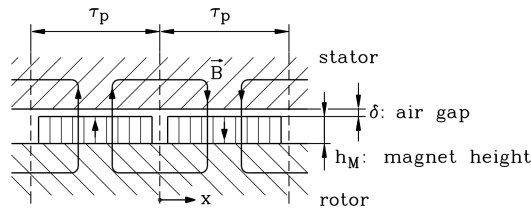


Fig. 9.16: Idealised flux distribution in a PM machine as a result of permanent magnet excitation at zero current

This magnetic “load line” (9.36) with negative slope is shown in Fig. 9.17, containing the points of operation  $P_1, P_2, P_3$  and  $P_4$ . The point of intersection with the  $B_M(H_M)$ -characteristic  $P$  is a function of the temperature  $T$ . The resultant flux density  $B_M$  decreases with increasing temperature of the magnets. It equals the flux density in the air gap of the machine  $B_\delta = B_p$ . It is **smaller** than the remanence flux density  $B_R$ , and it is decreasing with increasing ratio “air gap/magnet height”.

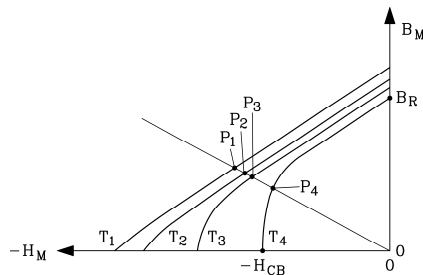


Fig. 9.17: Magnetic operating point  $P$  of a permanent magnet synchronous machine at zero current as a function of temperature  $T_1 < T_2 < T_3 < T_4$ .

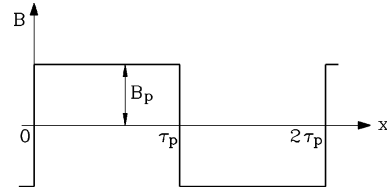


Fig 9.18: Air gap flux density of a permanent magnet synchronous machine (idealised) with N- and S-pole

The idealised field distribution  $B_p(x)$  in the air gap as a result of surface mounted permanent magnets is rectangular, if the influence of the gap between neighbouring magnet poles is neglected. If only the sinusoidal fundamental of this flux distribution is considered, the phasor diagram of Chapter 8 can also be used for these PM synchronous machines. In this case, a

fictitious constant exciting current  $I_f$  is used as equivalent parameter for excitation of the PM flux density  $B_p$ .

**Result:**

Due to  $\mu_M \equiv \mu_0$ , the reactance of the stator field for longitudinal and quadrature axis are equal:  $X_d = X_q$ , so that permanent magnet machines with surface mounted magnets can be considered as round rotor machines.

**9.5.3 Inverter-Fed PM Synchronous Machines with Rotor Position Control**

Large, electrically excited synchronous machines, but also small permanent magnet synchronous machines are often operated via an inverter. Thereby, the stator winding is supplied with current, depending on the rotor position, and the stator field maintains a **constant relative position to the rotor**. The rotor position is measured by use of a **rotor position encoder**, e.g. an **incremental encoder** or a **resolver**.

In Fig. 9.19, the *principle of operation with rotor position measurement* is shown, simplified for a two-pole salient pole machine. The inverter considered here operates from a dc link with 6 power switches (e.g. thyristors, GTOs, IGBTs, ...). If the power switches 3 and 5 are conducting, exciting flux lines of the stator field  $B_s$ , which are spatially perpendicular to the rotor field. A mere quadrature field is obtained, because it is oriented in the  $q$ -axis of the rotor. The resultant motor torque has its maximum value. After a sixth of a period later, the rotor has turned by  $60^\circ$ . The rotor position encoder controls the inverter, so power switches 3 and 4 are conducting, thereby tracking the stator field, so that it is again perpendicular to the rotor field.

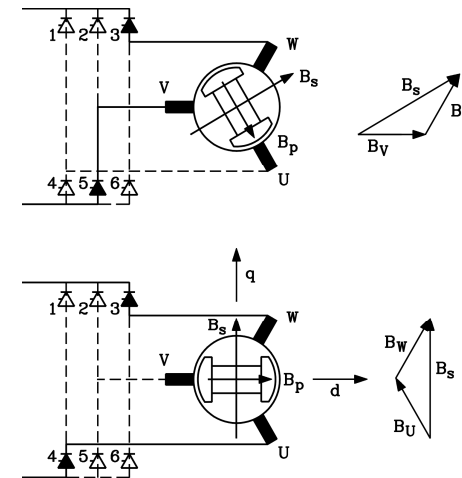


Fig. 9.19: Rotor position control: Maximum possible torque is obtained for all rotor positions by generating a stator field perpendicular to the rotor field, shown for two different rotor positions.

The direction of the flux linkage phasor  $\underline{\Psi}_p$  of the permanent magnet field  $B_p$  with the stator winding is defined as the  $d$ -axis (Fig. 9.20). It can be represented by a fictitious exciting current  $I_{fM}$ . The stator current must be supplied as  **$q$ -component current  $I_s = I_q$**  to obtain a stator field perpendicular to the rotor field (self-induced voltage  $jX_d I_s$  phase shifted by  $90^\circ$  to  $\underline{U}_p$ ). It is obvious from the corresponding Fig. 9.21, which shows the relative position of the

stator currents to the rotor magnets, that this position delivers maximum torque for a given current. All conductors with positive current direction are exposed to the north pole magnets. So the generated *LORENTZ* forces of all currents act into the same direction.

So, the same situation as **with dc machines** is obtained: In dc machines, the brushes slide on the commutator, thereby maintaining a constant relative position with respect to the stator poles. Thus, the electric currents have a constant position with respect to the stator field. The same situation is given for the machine operation shown in Fig. 9.21. Here, the *inverter* takes the role of the mechanical *commutator*, the *stator three-phase winding system* corresponds to the *dc-armature winding* of the dc rotor. The *rotor magnetic poles* of the PM synchronous machine correspond to the *dc-stator poles*, which may be also excited by permanent magnets in the case of small dc-machines. Therefore, rotor position controlled synchronous machines are called "**brushless dc-machines**".

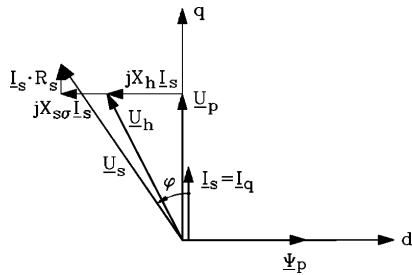


Fig. 9.20: Phasor diagram of Fig. 9.19 for maximum possible torque (motor operation)

As the stator current phase shift is impressed by the inverter in dependence of the rotor position via the stator voltage, this voltage is no longer a constant value, but has to be adjusted to the appropriate value by the inverter (Fig. 9.20). The torque-load angle characteristic of a synchronous machine that is operated at a constant voltage (Chapter 8) is no longer valid. The machine cannot be pulled out of synchronism any more, because the rotor position control directly tries to "catch" the rotor. Details to this PM drive technology see lecture "*Motor Development for Electrical Drive Systems*".



Fig. 9.22: One-arm-robot with permanent magnet synchronous machines used as drives

9.6 Starting and Synchronisation of Synchronous Machines

Starting and connecting of a synchronous machine to the line ("**synchronisation**") are also dynamic incidents.

a) *Generators:*

Generators are usually driven with excited rotor by the **turbine** up to rated speed (hence the induced stator back-e.m.f. has rated frequency) and are then **synchronised**.

**Synchronisation:**

- The amplitude of the induced stator voltage at no load (back-e.m.f.  $U_p$ ) is adjusted by  $I_f$  to equal the amplitude of the line voltage  $U_s$ .
- The voltage phase angle and phase sequence U,V,W of  $U_p$  must equal those of the three-phase system  $U_s$  of the line. Then, the machine can be connected to the grid without occurrence of a transient compensating current peak.

If these requirements are not met (synchronisation failure), compensating currents similar to short circuit currents occur, resulting in large current peaks and pulsating torque.

In **pump storage power stations**, the synchronous machine has to operate as generator and as motor, and the starting may be performed **asynchronously** via the damper cage. The damper cage must be designed to allow for this (**starting cage**), because the copper losses occurring in the damper cage during starting equal the kinetic energy stored in the drive. Furthermore, like with induction motors, synchronous machines running up with a starting cage have large start-up stator currents that may lead to a sag of the line voltage. Therefore, often a small **start-up turbine** or an **auxiliary motor** is used for running up the coupled synchronous machine. Alternatively, the generator can be started as a motor via a **start-up inverter** that supplies the stator winding with variable frequency.

b) *Motors:*

**Inverter-fed synchronous motors** (e.g. in steel-mills, compressor stations,...) are started with variable speed from the line via the feeding inverter. Further information on these **large drives** is given in the lecture "*Large generators and high power drives*".

**Line-fed synchronous motors** are either started asynchronously via a starting cage, an auxiliary motor or a start-up inverter. If the voltage sag resulting from the big starting current during asynchronous running up is too large, a **starting transformer** or a **starting reactor** is used.

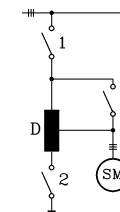


Fig. 9.23: Start-up connection using three switches according to KORNDÖRFFER (D: start-up reactor, SM: synchronous machine)

Start-up connection according to KORNDÖRFFER using a starting reactor (Fig. 9.23):

**Step 1:** Switches 1 and 2 are closed, switch 3 is open: The reactor D acts as a voltage divider. The synchronous motor runs up at reduced voltage. This increases the running up time, but decreases the starting current.

Step 2: Switch 2 is also opened: The part of the winding of the reactor between 1 and 3 acts as external impedance in the supply of the stator winding and limits the current.

Step 3: Switch 3 is closed: The synchronous motor is connected to full voltage.

*Result:*

*The current in the stator winding has not been interrupted during running up, but was reduced.*

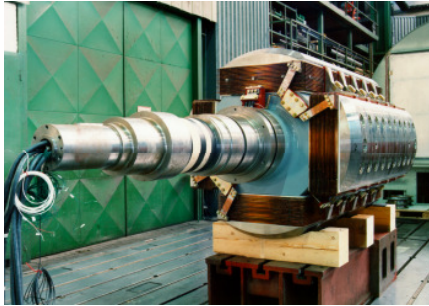


Fig. 9.24: Four pole salient pole synchronous motor with massive iron rotor poles for asynchronous line start: Instead of a starting cage the rotor current is induced by the stator field in the massive conducting rotor iron pole shoes. The pole shoe eddy currents generate in combination with the stator air gap field the starting torque. The advantage is the better heat transfer of the rotor pole shoe losses to the adjacent air, compared to the cage solution (Source: VAtech Hydro, Austria)